$B \to \rho K^*$ decays and other rare vector-vector modes *

G. Vasseur†
DSM/DAPNIA/SPP, CEA/Saclay, F-91191 Gif-sur-Yvette, France

The recent analyses of the following rare vector-vector decays of the B meson are presented: ρK^*, ωK^*, $\omega\rho$, $\omega\omega$, and $\omega\phi$ charmless final states. The latest results indicate that the fraction of longitudinal polarization is about 0.5 in penguin-dominated modes and close to 1 for tree-dominated modes.

I. MOTIVATION

The search for rare charmless hadronic decays of the B meson to vector-vector final states has become a quite active field in the experiments at the B factories, Belle at KEK and *BABAR* at SLAC. As a lot of these decays have not yet been seen, the first goal of these studies is to observe such modes and measure their branching fraction. The measurements can then be compared to theoretical predictions.

The direct CP-violation asymmetry in these modes can also be measured. It is defined as $\mathcal{A}_{\rm CP} = (\Gamma^- - \Gamma^+)/(\Gamma^- + \Gamma^+)$, where the superscript on the total width Γ indicates the sign of the b-quark charge in the B meson. Some modes can be used for further CP studies. In fact, the result on $B^+ \to \rho^+ K^{*0}$ has already been used to constrain the effect of the penguin amplitude on the measurement of the angle α of the unitarity triangle from $B^0 \to \rho^+\rho^-$ using SU(3) flavor symmetry [1].

A hot topic is the measurement of the fraction of longitudinal polarization. The helicity angles θ_1 and θ_2 of the two vector mesons are defined as the angles between the vector meson direction in the B meson rest frame and the direction of one of its decay product in the vector meson rest frame, as illustrated on one example in Fig. 1. Integrating over the ϕ angle between the decay planes of the two vector mesons, the fraction of longitudinal polarization f_L can be extracted from the angular dependence of the decay rate, which is proportional to

$$\frac{1}{4}(1-f_L)\sin^2\theta_1\sin^2\theta_2 + f_L\cos^2\theta_1\cos^2\theta_2.$$

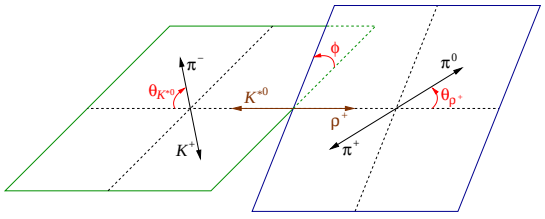

FIG. 1: Definition of the helicity angles in the case of the vector-vector $B^+ \to \rho^+ K^{*0}$ decay.

A value of f_L close to unity of order $(1-O(\frac{{m_V}^2}{{m_B}^2}))$ is expected for light vector mesons from helicity conservation. This is expected to be true for both tree and penguin diagrams. However the experimental situation is more complex. If f_L has indeed been measured close to 1 in the tree-dominated $B \to \rho\rho$ modes [2], it is surprisingly close to 0.5 in the penguin-dominated $B \to \phi K^*$ modes [3]. This effect is not yet understood. There are several possible explanations, either within the Standard Model, such as rescattering in the final state, contribution from annihilation or electroweak penguin diagrams, and transverse gluon [4], or in new physics outside the Standard Model. To have a better picture, it is important to measure other vector-vector modes, both tree-dominated, like $B \to \omega\rho$ and $B^0 \to \omega\omega$, and penguin-dominated like $B \to \rho K^*$ and $B \to \omega K^*$.

The recent studies of the $B \to \rho K^*$ modes are reviewed in section II, the ones involving an ω meson in section III. Charge-conjugate modes are implied throughout.

II. $B \to \rho K^*$ MODES

A. Introduction

The $B \to \rho K^*$ charmless decays proceed through dominant gluonic penguin loops and doubly Cabibbo-suppressed tree processes, as shown in Fig. 2. The external tree diagram is only possible with a K^{*+}, and the color-suppressed internal tree diagram with a ρ^0. Hence $B^+ \to \rho^+ K^{*0}$ is pure penguin.

According to isospin symmetry, the two modes with a charged ρ are expected to have a branching fraction twice as large as the two modes with a neutral ρ.

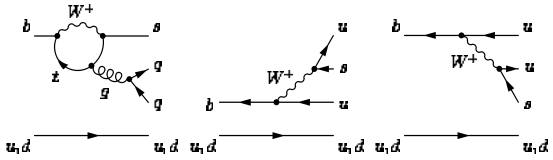

FIG. 2: Feynmann diagrams for the $B \to \rho K^*$ decay: gluonic penguin, external tree and internal tree diagrams.

*Presented at the 4^{th} International Workshop on the CKM Unitariry Triangle, Nagoya, Japan, December 12-16, 2006.

†Electronic address: georges.vasseur@cea.fr

B. Results from Belle

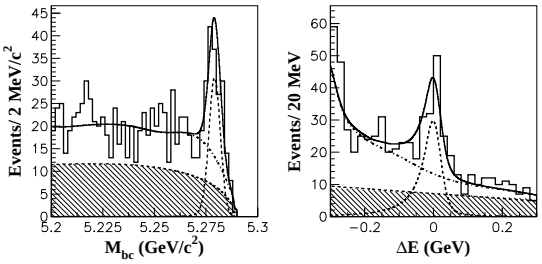

FIG. 3: Projections of M_{bc} for events in the ΔE signal region (left) and of ΔE in the M_{bc} signal region (right). The solid curves show the results of the fit. The dashed curve is the signal contribution. The hatched histograms represent the continuum background. The sum of the $b \to c$ and continuum background component is shown as dot-dashed lines.

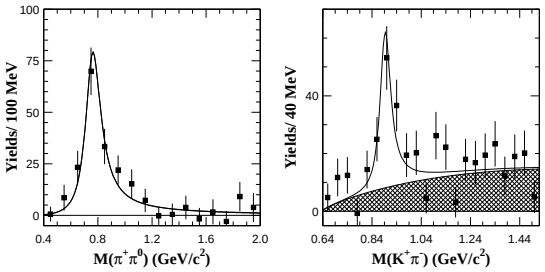

FIG. 4: Signal yields obtained from the M_{bc}-ΔE distribution in bins of $M(\pi^+\pi^0)$ (left) for events in the K^{*0} region and in bins of $M(K^+\pi^-)$ (right) for events in the ρ^+ region. The points with error bars show the data. Solid curves show the results of the fit. Hatched histograms are for the nonresonant component.

Belle was the first experiment in 2005 to publish a result on the observation of the $B^+ \to \rho^+ K^{*0}$ mode [5], on a sample of 275 millions of $B\bar{B}$ pairs. A signal of $B^+ \to \pi^+\pi^0 K^+\pi^-$ is extracted from the $e^+e^- \to q\bar{q}$ continuum and $B\bar{B}$ backgrounds in an extended unbinned maximum-likelihood fit using the B meson beam-constrained mass M_{bc} and energy difference ΔE, as shown in Fig 3.

The $B^+ \to \rho^+ K^{*0}$ signal is extracted by fits to M_{bc} and ΔE in bins of the vector meson masses $M(\pi^+\pi^0)$ and $M(K^+\pi^-)$, as shown in Fig 4. This is necessary because there is a large nonresonant $\rho K\pi$ background, which gives a continuum in the distribution of $M(K^+\pi^-)$. Nethertheless there is a clear $B^+ \to \rho^+ K^{*0}$ signal of 85 ± 16 events with a significance of $5.2\ \sigma$.

As for f_L, it is obtained by fitting simultaneously the signal yields obtained from M_{bc}-ΔE fits in bins of the two helicity angles, assuming an S-wave $K\pi$ system in the $\rho K\pi$ background. The results for the branching fraction and f_L in $B^+ \to \rho^+ K^{*0}$ are:

$$\begin{aligned} \mathcal{B} &= (8.9 \pm 1.7 \pm 1.2)\, 10^{-6}, \\ f_L &= 0.43 \pm 0.11^{+0.05}_{-0.02}. \end{aligned}$$

The value found for f_L is similar to the one found in ϕK^* and its error is about twice as large as in ϕK^*.

C. Results from *BABAR*

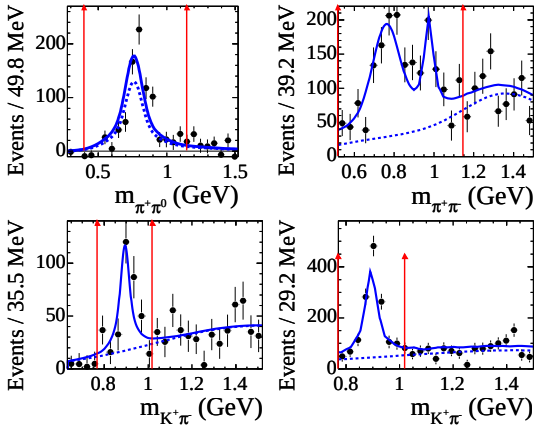

FIG. 5: sPlots for the $\pi\pi$ (top) and $K\pi$ (bottom) invariant masses in the $B^+ \to \rho^+ K^{*0}$ (left) and $B^0 \to \rho^0 K^{*0}/B^0 \to f_0(980)K^{*0}$ (right) analyses. The points with error bars show the data. The solid curve shows the signal and nonresonant background contribution, the dashed curve is the nonresonant background contribution ($\rho K\pi$ except for the top right plot where it represents the sum of $f_0(1370)K^*$, $\pi\pi K^*$, and $\pi\pi K\pi$). The arrows show the standard mass windows used in the final fit.

More recently *BABAR* published an anlysis of all four $B \to \rho K^*$ modes [6], performed on a sample of 232 millions of $B\bar{B}$ pairs. It is based on an unbinned maximum-likelihood fit, using seven variables: the B meson energy-substituted mass m_{ES} and energy difference ΔE, a neural network output or a Fischer discriminant combining several event shape variables, the two vector meson masses, and the two helicity angle cosines. The fit allows the simultaneous extraction of the branching ratio and the fraction of longitudinal polarization.

The major challenge in the analysis comes from the nonresonant backgrounds, which share the same final state as the signal. They are studied by enlarging the vector meson mass windows, as illustrated in Fig. 5. As in Belle, a large $\rho K\pi$ background is seen in the $m_{K\pi}$ distribution in the $B^+ \to \rho^+ K^{*0}$ mode. The $K\pi$ system in this background is measured to be mostly S-wave. The situation is even more complex in the $B^0 \to \rho^0 K^{*0}$ mode, since in addition to the $\rho K\pi$ background there are several contributions seen in the $m_{\pi\pi}$ distribution for a ρ^0 in contrast to the one for a ρ^+. The $f_0(980)$ can be seen clearly. In fact $B \to f_0(980)K^*$, which is a scalar-vector

TABLE I: Results from *BABAR* on the $B \to \rho K^*$ modes: signal yield with its statistical uncertainty, significance (systematic uncertainties included), branching fraction (90% confidence level upper limit in parentheses), fraction of longitudinal polarization and direct CP asymmetry. (The numbers in brackets are not quoted as measurements.)

Mode	Signal yield	Significance (σ)	B($\times 10^{-6}$)	f_L	$\mathcal{A}_{CP}$
$B^+ \to \rho^0 K^{*+}$	51 ± 24	2.5	$< 6.1\,(3.6 \pm 1.7 \pm 0.8)$	$[0.9 \pm 0.2]$	
$B^0 \to \rho^- K^{*+}$	60 ± 24	1.6	$< 12.0\,(5.4 \pm 3.6 \pm 1.6)$		
$B^+ \to \rho^+ K^{*0}$	194 ± 29	7.1	$9.6 \pm 1.7 \pm 1.5$	$0.52 \pm 0.10 \pm 0.04$	$-0.01 \pm 0.16 \pm 0.02$
$B^0 \to \rho^0 K^{*0}$	185 ± 30	5.3	$5.6 \pm 0.9 \pm 1.3$	$0.57 \pm 0.09 \pm 0.08$	$0.09 \pm 0.19 \pm 0.02$

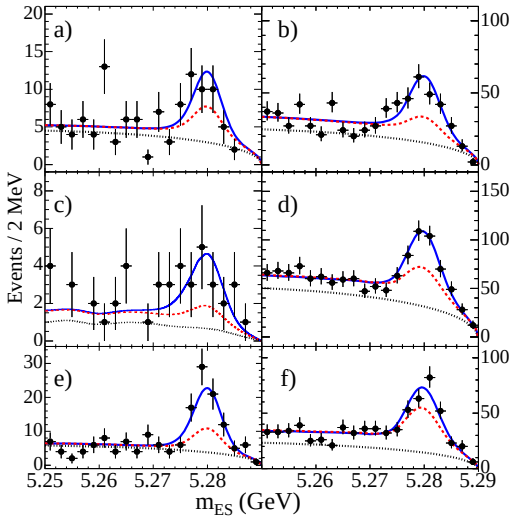

FIG. 6: Projections of m_{ES} of events passing a signal likelihood threshold for (a) $B^+ \to \rho^0 K^{*+}$, (b) $B^+ \to \rho^+ K^{*0}$, (c) $B^0 \to \rho^- K^{*+}$, (d) $B^0 \to \rho^0 K^{*0}$, (e) $B^+ \to f_0(980) K^{*+}$, and (f) $B^0 \to f_0(980) K^{*0}$. The points with error bars show the data. The solid curve is the fit function, the dashed curve is the total background contribution, and the dotted curve is the continuum background contribution.

mode, is considered as another signal to be measured in the same maximum-likelihood fit. Also present are contributions from the $f_0(1370)$ and nonresonant $\pi\pi$. The yields of the nonresonant backgrounds are fitted in the enlarged mass windows, then extrapolated to the standard ones and fixed in the final fit with the standard mass windows.

The projection plots in the B mass shown in Fig. 6 illustrate the extraction of the signal from the continuum and $B\bar{B}$ backgrounds in the four $B \to \rho K^*$ channels and the two $B \to f_0(980) K^*$ modes. Table I summarizes the results. No significant enough signals are observed for $B^0 \to \rho^- K^{*+}$ and $B^+ \to \rho^0 K^{*+}$, where upper limits at the 90 % confidence level are set on the branching ratios. For the latter a related signal $B^+ \to f_0(980) K^{*+}$ is observed with a significance of $5.0\,\sigma$ and a measured branching fraction of $(5.2 \pm 1.2 \pm 0.5)\,10^{-6}$. In $B^+ \to \rho^+ K^{*0}$, the result is in very good agreement with the result from Belle, with a similar precision. The $B^0 \to \rho^0 K^{*0}$ mode is observed for the first time. The ratio between the branching fractions in these two modes is compatible with the factor 2 expected from isospin symmetry.

The value of $\mathcal{A}_{CP}$ is measured in the two significant modes to be compatible with 0, as expected since there is one dominant diagram. Finally f_L is found close to 0.5 in these two modes. It is compatible with the measurement from Belle and has about the same precision. It is again similar to the value found for ϕK^*.

III. MODES WITH ω

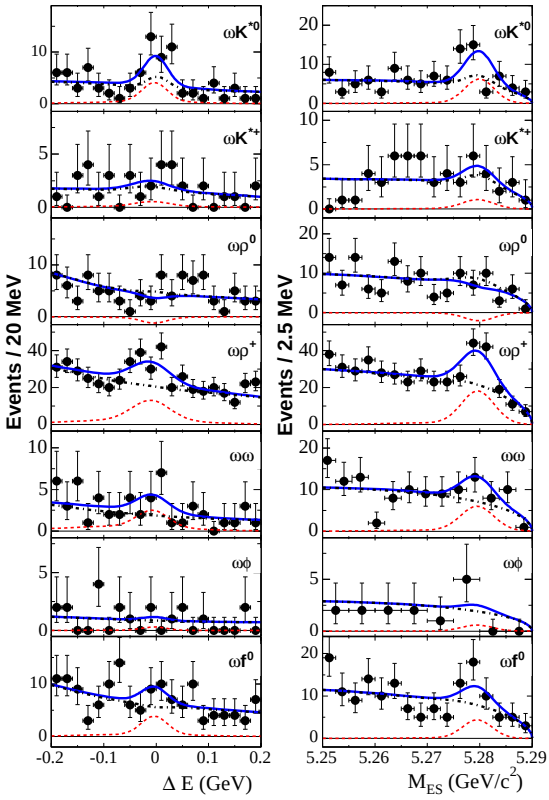

FIG. 7: Projections of ΔE (left) and m_{ES} (right) of events passing a signal likelihood threshold for, from top to bottom, $B^0 \to \omega K^{*0}$, $B^+ \to \omega K^{*+}$, $B^0 \to \omega \rho^0$, $B^+ \to \omega \rho^+$, $B^0 \to \omega\omega$, $B^0 \to \omega\phi$, and $B^0 \to \omega f_0(980)$. The points with error bars show the data. The solid curve is the fit function, the dashed curve is the signal contribution, and the dot-dashed curve is the background contribution.

TABLE II: Results from *BABAR* on modes involving an ω meson: signal yield with its statistical uncertainty, significance (systematic uncertainties included), branching fraction (90% confidence level upper limit in parentheses), fraction of longitudinal polarization and direct CP asymmetry. (The numbers in brackets are not quoted as measurements.)

Mode	Signal yield	Significance (σ)	B($\times 10^{-6}$)	f_L	$\mathcal{A}_{CP}$
$B^0 \to \omega K^{*0}$	55 ± 20	2.4	$< 4.2\ (2.4 \pm 1.1 \pm 0.7)$	$[0.71 \pm 0.25]$	
$B^+ \to \omega K^{*+}$	8 ± 16	0.4	$< 3.4\ (0.6 \pm 1.3 \pm 1.0)$		
$B^0 \to \omega \rho^0$	-18 ± 16	0.6	$< 1.5\ (-0.6 \pm 0.7^{+0.8}_{-0.3})$		
$B^+ \to \omega \rho^+$	156 ± 32	5.7	$10.6 \pm 2.1^{+1.6}_{-1.0}$	$0.82 \pm 0.11 \pm 0.02$	$0.04 \pm 0.18 \pm 0.02$
$B^0 \to \omega\omega$	48^{+24}_{-19}	2.1	$< 4.0\ (1.8^{+1.3}_{-0.9} \pm 0.4)$	$[0.71 \pm 0.25]$	
$B^0 \to \omega\phi$	$3.1 \pm ^{+4.4}_{-8.5}$	0.3	$< 1.2\ (0.1 \pm 0.5 \pm 0.1)$		

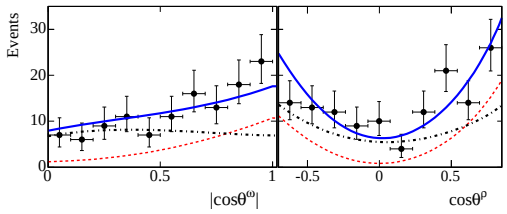

FIG. 8: Projections of the helicity-angle cosines for ω (left) and ρ^+ (right) of events passing a signal likelihood threshold from the fit for $B^+ \to \omega\rho^+$ decays. The points with error bars show the data. The solid curve is the fit function, the dashed curve is the signal contribution, and the dot-dashed curve is the background contribution.

On the same sample of 232 millions of $B\bar{B}$ pairs, *BABAR* has also recently published a search for several vector-vector modes involving an ω meson [7]: $B^0 \to \omega K^{*0}$, $B^+ \to \omega K^{*+}$, $B^0 \to \omega\rho^0$, $B^+ \to \omega\rho^+$, $B^0 \to \omega\omega$, and $B^0 \to \omega\phi$. The related vector-scalar mode $B^0 \to \omega f_0(980)$ was also searched for. An earlier search for $B \to \omega K^*$ and $B \to \omega\rho$ on 89 millions of $B\bar{B}$ pairs resulted in the first observation of the $B^+ \to \omega\rho^+$ channel [8].

The analysis is also based on an extended unbinned maximim-likelihood fit using the same seven variables as in the previous section. Nonresonant $\pi\pi$ and $K\pi$ backgrounds are fixed in the fit as determined from extrapolations from higher-mass regions. The projection plots of ΔE and m_{ES} of Fig. 7 illustrate the extraction of the signal from the continuum and $B\bar{B}$ backgrounds in all these modes. In most of them, no significant enough signal is seen. The only channel where a significant signal is observed is $B^+ \to \omega\rho^+$. Its measured branching fraction is about 2 standard deviations smaller than the one of $B^+ \to \rho^+\rho^0$ [2], while these two branching fractions are naively expected to be equal. Table II summarizes the results in all the modes. To calculate the branching fraction, f_L is left free in the fit for the three modes with a signal significance greater than 2σ and is fixed otherwise. Upper limits at the 90 % confidence level are set on the branching fractions for the modes other than $B^+ \to \omega\rho^+$.

The maximum-likelihood fit also provides the value of f_L in $B^+ \to \omega\rho^+$, which is found to be 0.82 ± 0.11, a high value expected for this tree-dominated mode. This is illustrared in the projection plots of the helicity angle cosines shown in Fig. 8. The direct CP asymmetry is also measured and found to be compatible with 0.

IV. CONCLUSION

In summary, improved analyses with explicit consideration of nonresonant backgrounds have been performed on several charmless hadronic vector-vector decays of the B meson. The $B^+ \to \omega\rho^+$, $B^+ \to \rho^+ K^{*0}$, and $B^0 \to \rho^0 K^{*0}$ modes have been observed and measured in the past few years. Improved upper limits have been set on the branching fraction of other vector-vector modes.

The recent results on vector-vector modes have also brought more pieces to the polarization puzzle. The penguin-dominated $B^+ \to \rho^+ K^{*0}$ and $B^0 \to \rho^0 K^{*0}$ modes have a fraction of longitudinal polarization of about 0.5 like ϕK^*, while the tree-dominated $B^+ \to \omega\rho^+$ mode has one closer to 1 like $\rho\rho$. As a lot of charmless vector-vector modes have not yet been observed, new results can be expected with more data.

[1] M. Beneke *et al.*, Phys. Lett. B **638**, 68 (2006).
[2] A. Somov, contribution to this conference.
[3] K.F. Chen, contribution to this conference.
[4] G.W.S. Hou, contribution to this conference.
[5] J. Zhang *et al.*, Phys. Rev. Lett. **95**, 141801 (2005).
[6] B. Aubert *et al.*, Phys. Rev. Lett. **97**, 201801 (2006).
[7] B. Aubert *et al.*, Phys. Rev. D **74**, 051102 (2006).
[8] B. Aubert *et al.*, Phys. Rev. D **71**, 031103 (2005).